https://dx.doi.org/10.1016/j.buildenv.2021.108590

Evaluation of different air distribution systems in a commercial airliner cabin in terms of comfort and COVID-19 infection risk

Mingxin Liu[a], Junjie Liu[a], Qing Cao[b], Xingyang Li[a], Sumei Liu[a,*], Shengcheng Ji[c], Chao-Hsin Lin[d], Daniel Wei[e], Xiong Shen[a], Zhengwei Long[a], Qingyan Chen[f]

[a] Tianjin Key Lab of Indoor Air Environmental Quality Control, School of Environmental Science and Engineering, Tianjin University, Tianjin 300072, China.

[b] School of Civil Engineering, Dalian University of Technology (DUT), 2 Linggong Road, Dalian, 116024, China Dalian University of Technology, Dalian, China

[c] Beijing Aeronautical Science & Technology Research Institute of COMAC, Beijing, China

[d] Environmental Control Systems, Boeing Commercial Airplanes, Everett, WA 98203, USA

[e] Boeing Research & Technology, Beijing 100027, China

[f] Department of Building Environment and Energy Engineering, The Hong Kong Polytechnic University, Hong Kong

ABSTRACT

The air distribution system in an airliner plays a key role in maintaining a comfortable and healthy environment in the aircraft cabin. To evaluate the performance of a novel displacement ventilation (DV) system and a traditional mixing ventilation (MV) system in an airliner cabin, this study conducted experiments and simulations in a seven-row cabin mockup. This investigation used ultrasonic anemometers and T-thermocouples to measure the air velocity, temperature and distribution of 1 μm and 5 μm particles. Simulation verifications were performed for these operating conditions, and additional scenarios with different occurrence source locations were also simulated. This study combined the Wells-Riley equation with a real case based on a COVID-19 outbreak among passengers on a long-distance bus to obtain the COVID-19 quanta value. Through an evaluation of the airflow organization, thermal comfort, and risk of COVID-19 infection, the two ventilation systems were compared. This investigation found that polydisperse particles should be used to calculate the risk of infection in airliner cabins. In addition, at the beginning of the pandemic, the infection risk with DV was lower than that with MV. In the middle and late stages of the epidemic, the infection risk with MV can be reduced when passengers wear masks, leading to an infection risk approximately equal to that of DV.

KEY WORDS

Airliner Cabin; Displacement Ventilation; Mixing Ventilation; Infection Risk; Thermal Comfort; Effect of Masks

Highlights

- This research compared the thermal and health characteristics of displacement and mixing ventilation systems in airliners.
- This investigation used the distribution of polydisperse particles to study infection risks.
- This paper addresses the impact of mask-wearing by passengers on infection risk with different ventilation systems in airliner cabins.

1. Introduction

The number of people choosing to travel by airliner is increasing [1]. In contrast with the typical environments inside public buildings, the environments of airliner cabins are narrow spaces with high occupant densities. Long periods of travel make passengers and crew members more sensitive to the cabin environment [2, 3]. The airborne transmission of infectious diseases has been reported in commercial aircraft, such as the transmission of influenza [4], tuberculosis [5], severe acute respiratory syndrome (SARS) [6], and coronavirus disease 2019 (COVID-19) [7-12]. Therefore, research on the indoor environments of airliner cabins is particularly important. A well-operated environmental control system (ECS) on an airliner can effectively remove pollutants and heat in the air and maintain a comfortable and healthy environment in the cabin [13-15]. Hence, the evaluation of different air distribution systems in airliner cabins is necessary.

Currently, mixing ventilation (MV) is commonly installed in a variety of airliners. This type of ventilation system cleans air with high-efficiency particulate air (HEPA) filters and supplies the air to the cabin through shoulder diffusers and/or ceiling diffusers, exhausting air through side diffusers near the floor of the cabin. Unfortunately, the heat rejection efficiency [16] and pollutant transmission control [17-20] of MV systems are not satisfactory. To provide a healthy and comfortable environment to passengers and crew members, a new type of ventilation system must be developed for airliner cabins. A superior system to MV is displacement ventilation (DV), which has been found to provide thermal comfort and good indoor air quality (IAQ) in buildings [21-24] and is widely used in other spaces such as train compartments [25]. Previous studies have demonstrated the ability of DV to provide a comfortable and healthy environment in airliner cabins [26-28]. Although there was a clear vertical temperature gradient for the DV systems, the air velocity was low in DV [27]. A more homogeneous cabin air flow was found in DV systems that led to improved thermal comfort for aisle seats [28]. In this type of ventilation, clean air is supplied through side diffusers near the floor of the cabin and exhausted through ceiling diffusers. Meanwhile, according to one previous study, among all MV systems (including those with only shoulder diffusers to supply air and only ceiling diffusers to supply air), an MV system in which shoulder diffusers and ceiling diffusers simultaneously supply air has the lowest air age and the highest heat rejection efficiency [16]. In comparison, DV has a higher heat rejection efficiency than all MV systems [16] and significantly reduces drafts [27-29]. However, the previous researches [27, 28] only conducted simple analysis on the flow field in airliner cabins, and could not

provide practical guidance for the selection of the air distribution systems. The only research by You et al. [26] can only provide guidance on the selection of air distribution systems in the early stages of the epidemic, and cannot compare the performance of air distribution systems in the middle and late stages of the epidemic.

Generally, the evaluation of ventilation systems includes two aspects: comfort and health. Comfort is assessed in terms of airflow organization and thermal comfort. The evaluation of airflow organization usually requires experimental study or simulations of the air distribution. Thermal comfort evaluation typically involves the assessment of predicted mean vote (PMV), predicted percent dissatisfaction (PPD) and local thermal comfort. In the past, however, research on airliner cabins mainly addressed PMV and PPD [13], with little attention paid to local thermal comfort. To evaluate the ability of a ventilation system to provide a healthy environment, particle or tracer gas measurements [13, 30] have generally been performed to obtain the distribution characteristics and removal efficiency of pollutants.

The characteristics of airflows and particle distributions in airliner cabins are usually determined by experimental measurements [31-34] and numerical simulations [35-38]. The air distribution affects the distribution of particles and spread of pathogenic microbial aerosol particles [39, 40]. Gupta et al. [41] used the deterministic and Wells--Riley equations to evaluate the infection risk in a twin-aisle, fully occupied aircraft cabin. You et al. [26] combined the Wells-Riley equation with computational fluid dynamics (CFD) in simulating the infection risks for passengers in airliner cabins with different air distribution systems and found that there had highest infection risks in MV systems. A previous study calculated the distributions of contaminants in airliner cabins and concluded that the distributions of contaminants under an MV system were relatively uniform, which is not conducive to the control of infectious diseases [29]. However, the simulation results were probably recognized to be right only after they were compared and verified with experimental measurements [42]. Currently, there is little experimental data on high-precision particle distributions in airliner cabins. Existing studies involve few measured points [2, 43] and have not fully demonstrated the concentration distributions of contaminants in a section of the cabin; therefore, it is difficult to compare the experimental results with simulated values. Moreover, research on only a single particle size [44] cannot fully reflect the characteristics of contaminants in airliner cabins. A previous study showed that 58% of influenza viruses were distributed on particles with an aerodynamic diameter ≥ 1 μm, and 42% on particles ≤ 1 μm [45]. Studies with multiple particle sizes can better demonstrate the particle distribution characteristics in airliner cabins. However, conducting solely experimental research is time consuming and labor intensive. Combining experimental investigation with simulation research allows more data to be obtained for a wide variety of cases.

During the COVID-19 epidemic, face masks were recommended by government health departments, and surgical-grade masks were widely used. The wearing of masks by passengers can effectively block the spread of the virus, thereby reducing the risk of COVID-19 infection. Masks can prevent the spraying of droplets by infected individuals, reduce the amounts and velocities of droplets, block virus-containing droplet nuclei, and prevent the wearer from inhaling these droplets. To analyze the impact of masks on the

risk of passenger infection in airliner cabins, existing studies have used the filtering efficiency of masks on particles [41]. However, the number of viruses present on particles varies with particle size. It is not accurate to consider only the efficiency of masks in filtering particles. Rather, the efficiency of masks in filtering viruses should be used directly.

To evaluate the performance of the MV and DV systems, this study used the Wells-Riley equation to obtain the quanta value based on an outbreak on a long-distance bus during the 2020 COVID-19 epidemic. As reported in this paper, the particle concentration (1 μm, 5 μm) distribution in a single-aisle airliner cabin mockup was measured under two ventilation systems, and CFD simulations were performed on this scenario and other cases. This study also compared MV and DV in terms of comfort and health. The results were used to evaluate contaminant transmission and thermal comfort performance under the two ventilation systems in airliner cabins.

2. Methods

2.1 Cabin mockup and ventilation systems

In this study, a single-aisle full-scale cabin mockup was built in a laboratory. Figure 1 is an interior view of the mockup. There were 7 rows with 42 seats in which 42 dummies were seated. The cabin floor was covered with carpet and equipped with light strips. Air of a certain temperature was supplied to the cabin mockup through an air conditioning system. The airflow rate in the cabin was 9.5 L/s per passenger in both DV and MV systems. The surface temperature of the dummies was 30 °C ± 1 °C, dummies with a uniform temperature were set according to the study from Liu et al. [46].

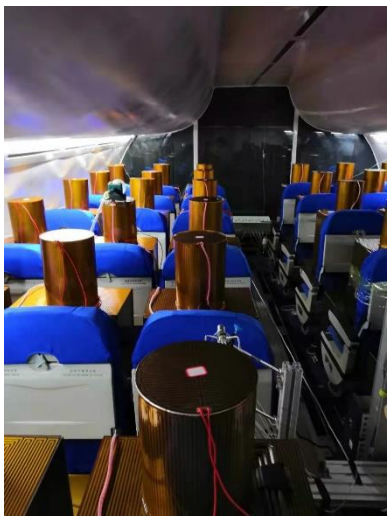

Figure 1 Interior of cabin mockup.

Figure 2 is a schematic diagram of the cabin mockup. The structural dimensions of the cabin mockup are detailed in Liu et al. [46]. The cabin mockup was ventilated by either of two ventilation systems, MV or DV, with identical airflow rates. The mixed ventilation system had 7 air supply diffusers on the ceiling, marked by ① in Figure 2, and their airflow rate accounted for 40% of the total air supply; there were 7 air supply diffusers on the shoulders on both sides, marked by ②, and their airflow rate accounted for 60% of the total air supply; and its exhaust diffusers were located on the lower parts

of both sidewalls near the floor, marked by ③ in Figure 2. In the DV system, air was supplied through diffusers in the lower parts of both sidewalls near the floor, marked by ③, and exhausted through diffusers in the ceiling, marked by ①.

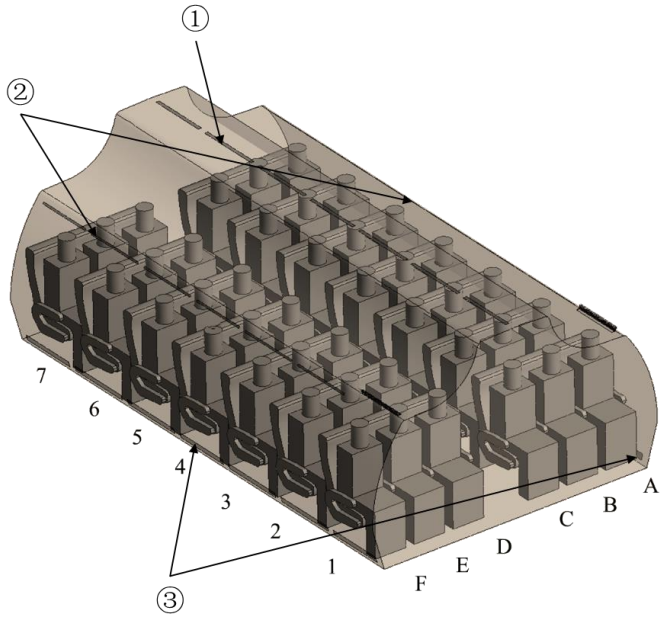

Figure 2 Schematic of a 7-row section of a fully occupied economy single-aisle airliner cabin

2.2 Experimental design

For evaluation of the transport of contaminants and the thermal comfort of passengers under different ventilation systems, the three-dimensional air velocity, air temperature and particle concentration distributions were measured in the cabin mockup. Ultrasonic anemometers were used to measure the air velocity in three directions, and T-thermocouples were used to measure the temperature. Particles were released by a polydisperse particle generator and measured by an aerodynamic particle size spectrometer. Table 1 shows the parameters of the instrument. Bioaerosols with a size between 1.0 and 5.0 μm generally remain in the air, while larger particles are quickly deposited on the surface [47, 48]. In this study, 1μm particles were selected to represent small-sized particles, and 5μm particles were selected to represent large-sized particles. If the particle size is larger, it may be trapped on the surface. This experiment focused on 1-μm and 5-μm particles, and the contaminant source was located at seat 4B. The particles were released from a small ball with a diameter of 8 cm, at a flow rate of 39 L/min. Point-by-point measurement of the particle concentration distribution began after the concentration in the exhaust pipe had stabilized. Before the measurements were taken, the system was allowed to run for 24 hours to ensure stable velocity and temperature distributions. The resolution of each measurement point was 150 mm × 150 mm, and the measurement section was the cross section in front of the fourth row of dummies. A previous study determined that passengers in this section would be at high risk of infection [26]. The specific experimental methods and instrument selection in the present study were identical to those of Liu et al. [46].

Table 1 *The parameters of the instrument*

Instrument	Model	Measurement range	Resolution	Accuracy
Ultrasonic anemometer	Kaijo Model DA-650 with TR-92T probe	0 ~ 10 m/s	0.005 m/s	±1%
Thermocouple	T-type	-10 ~ 40°C	0.02 K	± 0.5 K
Aerodynamic particle size spectrometer	APS-3321	0.5 ~ 20 μm; 0 ~ 1000 P/cm^3	0.001 P/cm^3	±10%

2.3 Simulation design

2.3.1 Calculation method

For accurate simulation of the velocity, temperature and particle concentration distributions in the cabin mockup, a suitable turbulence model was required. The realizable k-ε model has been proved to be the most effective and economical model for simulating airflows in the enclosed spaces of airliner cabins [49, 50].

To simulate the transport of particles in the cabin mockup, this study used the Lagrangian method, as shown in formula (1):

$$\frac{d\overrightarrow{u_p}}{dt} = \frac{18\mu}{\rho_p d_p^2 C_c}\left(\vec{u} - \overrightarrow{u_p}\right) + \frac{g(\rho_p - \rho)}{\rho_p} + \vec{F}_b + \vec{F}_{therm} + \vec{F}_s \quad (1)$$

where $\overrightarrow{u_p}$ is the particle velocity (m/s), t is the time (s), μ is the air viscosity (Pas), ρ_p is the particle density (kg/m^3), d_p is the particle diameter (m), C_c is the Cunningham correction factor, $\vec{u}$ is the air velocity (m/s), g is the acceleration of gravity (m/s^2), ρ is the air density (kg/m^3), $\vec{F}_b$ is the Brownian force (N), $\vec{F}_{therm}$ is the thermophoretic force (N), and $\vec{F}_s$ is the Saffman force (N).

2.3.2 Simulation design

Table 2 lists the boundary conditions in the CFD simulation, which were defined according to the measurement data. In the simulations, the residuals represented relative errors in the calculation of a particular variable. The solutions were considered to have converged when the sum of the residuals was less than 10^{-3}, 10^{-3} and 10^{-6}, respectively, for the continuity, momentum and energy equations. A standard wall function was used in the simulation. The computational domain was the air domain.

In the simulation, the particle source was generated in front of the dummy's head (4A, 4B, 4C), and particle sizes of 1 μm and 5 μm were selected. Reflective wall surfaces were employed as the wall boundary type, which means that particles would bounce off the boundary as the momentum changes [51].

Table 2 *Boundary conditions for the CFD simulation*

	Boundary parameter	Conditions
Wall	Constant temperature	Measurement data, divided into 15 areas [46]
Seat	Constant heat flux	0
Dummy	Constant temperature	30.1 °C

Air supply diffusers	Velocity-inlet	Measurement data, one diffuser divided into 7 parts
Air exhaust diffusers	Outflow	—
Particle	—	1 μm, 5 μm

2.3.3 Grid-independence study

According to a mesh-independence study, the difference in average outlet velocity for cases with 9 and 14 million elements was 1.32%, and the corresponding value for the difference in average outlet temperature between these two grid resolutions was 0.89%. Because the difference between the output results of the numerical simulations with grid sizes of 9 and 14 million elements was small, a grid size of 9 million was selected for the remainder of the study. The minimum element size was 10 mm and was located at the air supply diffusers. Figure 3 shows the distribution of the grid for the MV and DV systems. The average y+ values of different walls were not exactly the same, which were in the range of 18.3–26.6.

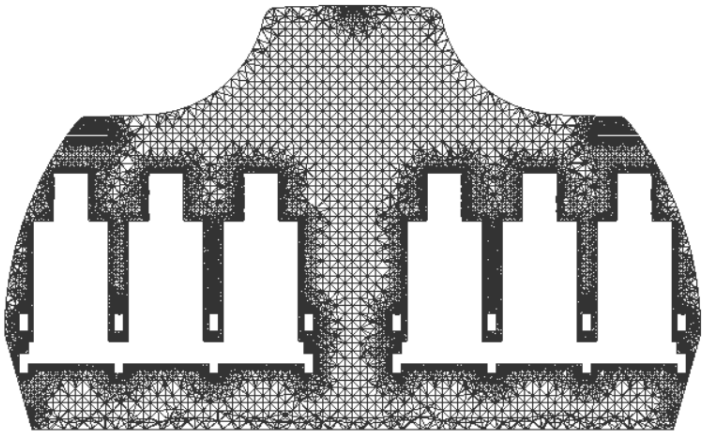

(a)

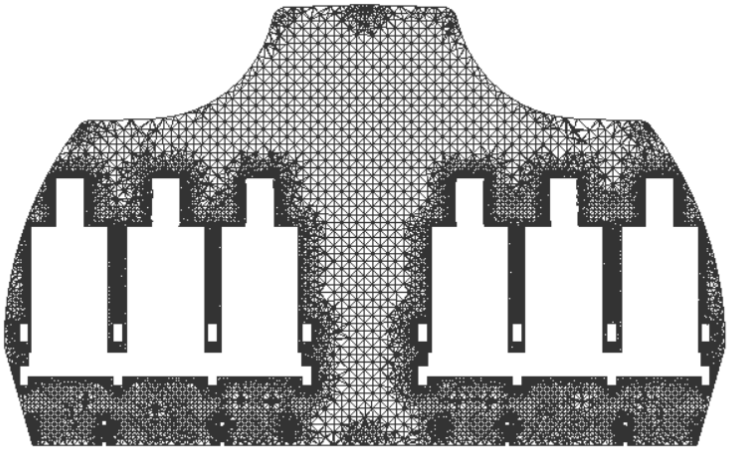

(b)

Figure 3 Distribution of the grid for (a) mixing ventilation and (b) displacement ventilation

2.3.4 Model validation

Figures 4 and 5 compare velocity vectors and velocity size in the experimental and simulated values of the MV and DV systems, respectively. The simulated air distribution exhibited some deviations from the experimental values, but the trends were identical. The results of an error analysis between simulated and experimental values at the measurement points are shown in Table 3. In comparison with the findings of a previous study [31], the simulated values in the present study were closer to the experimental values, probably because of the fine calibration of the air supply boundary [46]. Although the relative deviation of velocity in the DV system exceeded 50%, the reference value of velocity under the DV system was low (< 0.1 m/s), and the absolute deviation of velocity was only 0.021 m/s. Compared with previous simulation results [31], these results indicate a significant improvement. There are several possible reasons for the relative deviation of velocity in the present study. In the MV system, since there were no resistance components in front of the supply diffusers, the velocity deviation between the experimental and simulated values was small. In contrast, the DV system exhibited the opposite trend. More resistance components were encountered by the air supply jet in the DV system than in the MV system. In the simulations, the resistance components could only be simplified to control the absolute error of the velocity within an acceptable range.

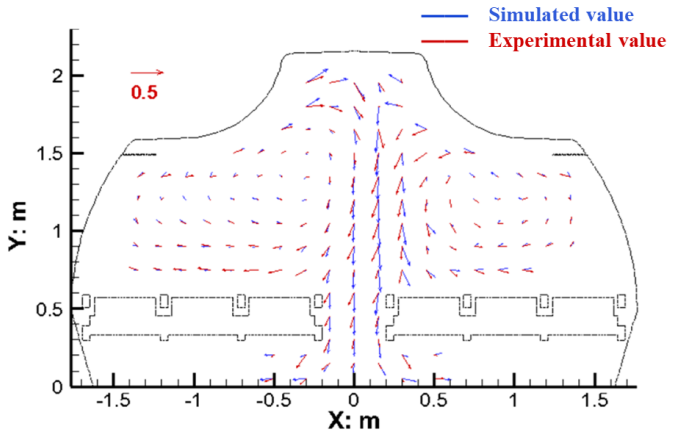

(a)

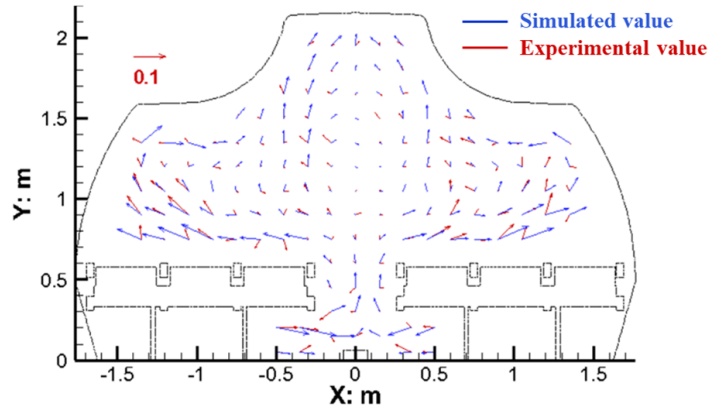

(b)

Figure 4 Comparison of the experimental and simulated values in the form of velocity vectors: (a) mixing ventilation and (b) displacement ventilation.

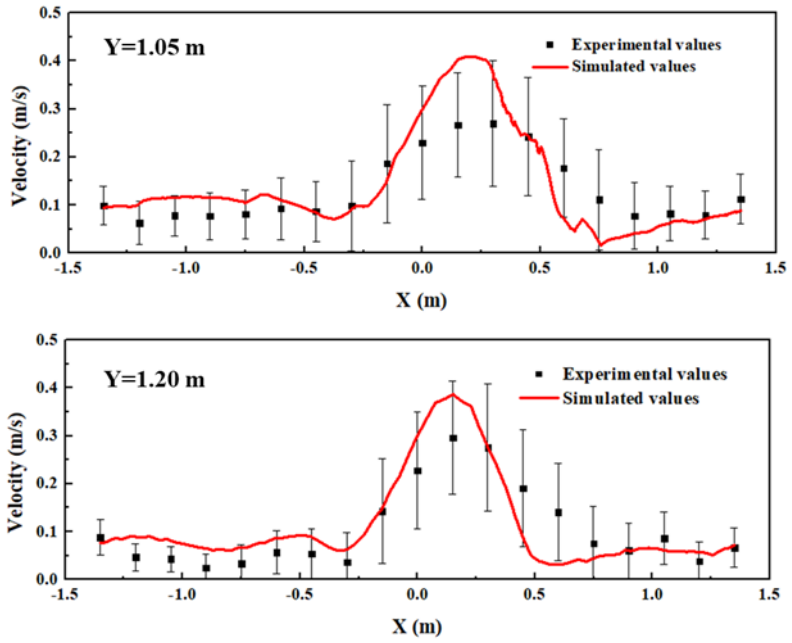

(a)

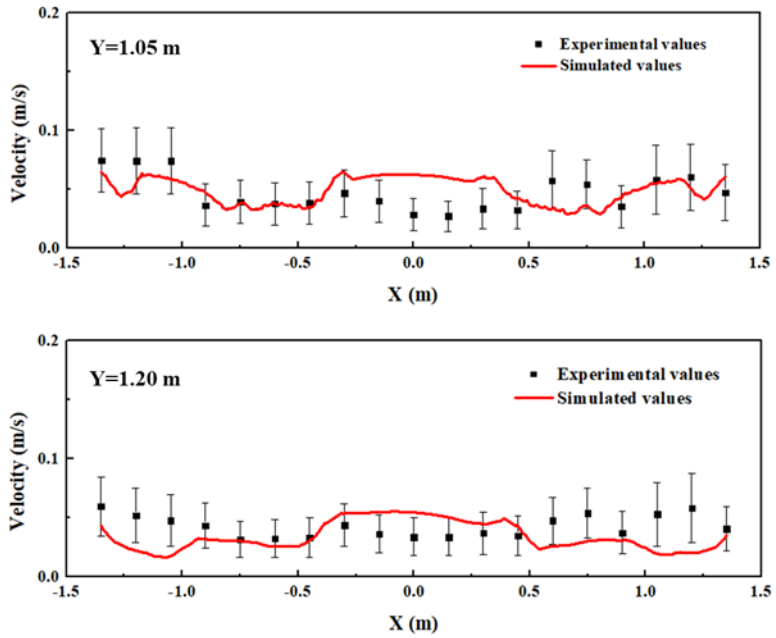

(b)

Figure 5 Comparison of the experimental and simulated velocity values: (a) mixing ventilation and (b) displacement ventilation.

The error analysis between the simulated and experimental values at the

measurement points is performed with the use of formulas (2) and (3) [31]:

$$Absolute\ deviation = \frac{\sum(U_{sim} - U_{exp})}{n} \quad (2)$$

$$Relative\ deviation = \frac{\sum(\frac{U_{sim} - U_{exp}}{U_{exp}})}{n} \times 100\% \quad (3)$$

where U_{sim} is the simulated value, velocity (m/s) or temperature (°C); U_{exp} is the experimental value, velocity (m/s) or temperature (°C); and n is the number of measurement points (-).

Table 3 *Error analysis between simulated and experimental values at the measurement points under different ventilation systems*

Ventilation system	Absolute deviation of velocity (m/s)	Relative deviation of velocity (%)	Absolute deviation of temperature (°C)	Relative deviation of temperature (%)
MV	0.008	5.644	0.82	3.280
DV	0.021	67.524	0.59	2.116
MD-82-MV [31]	0.052	113.300	0.9	3.820

Simulations were performed for 1-μm and 5-μm particles. A previous study showed that 58% of influenza viruses were distributed on particles with an aerodynamic diameter ≥ 1 μm, and 42% on particles ≤ 1 μm [45]. Therefore, this investigation calculated the infection risk by 58% of particle concentration with 5 μm, and 42% of particle concentration with 1 μm. Considering the concentration distributions of the two particle sizes, the calculated infection rate was compared with the infection rate determined from the experimental results (as shown in Figure 6), and the overall trend was essentially the same in both cases.

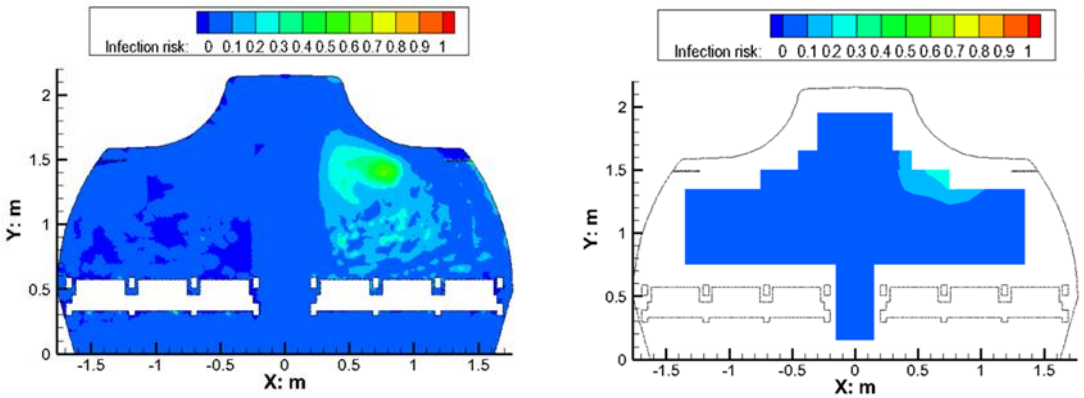

(a) *(b)*

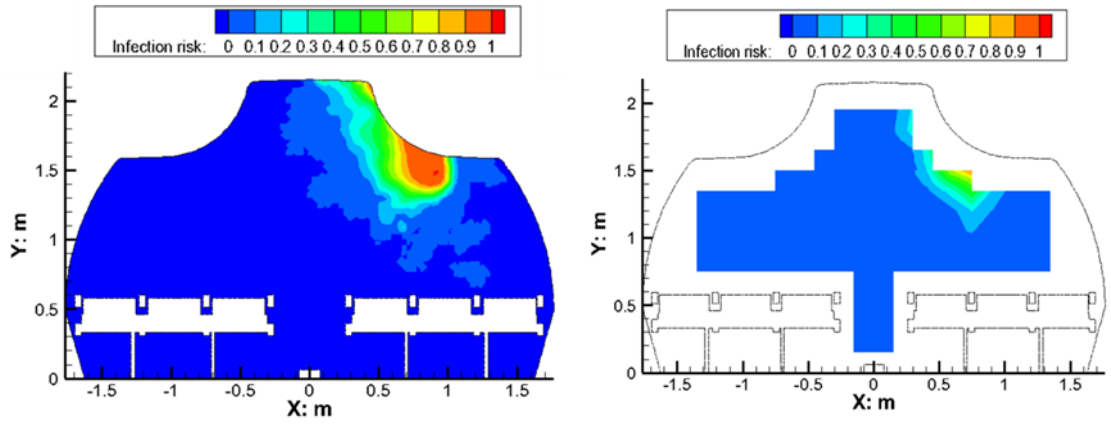

(c) *(d)*

Figure 6 Comparison of the experimental and calculated values of the infection risk: (a) simulated values under MV; (b) experimental values under MV; (c) simulated values under DV; (d) experimental values under DV.

2.4 Comfort evaluation

2.4.1 Airflow evaluation

The velocity nonuniformity index (VUI) [16] is used to quantitatively analyze the distribution characteristics of the air velocity in airliner cabins and are calculated as follows:

$$\overline{v} = \frac{\sum v_i}{n} \tag{4}$$

$$\delta_v = \sqrt{\frac{\sum(\overline{v}-v_i)^2}{n}} \tag{5}$$

$$VUI = \frac{\delta_v}{\overline{v}} \tag{6}$$

where n is the number of measurement points (-), v_i is the time-averaged velocity at each point (m/s), and $\overline{v}$ is the area-averaged velocity for all measurement points (m/s).

The temperature nonuniformity index (TUI) [16] is used to quantitatively analyze the distribution characteristics of the temperatures in airliner cabins and are calculated as follows:

$$\overline{T} = \frac{\sum T_i}{n} \tag{7}$$

$$\delta T = \sqrt{\frac{\sum(\overline{T}-T_i)^2}{n}} \tag{8}$$

$$TUI = \frac{\delta T}{\overline{T}} \tag{9}$$

where T_i is the time-averaged temperature at each point (°C), and $\overline{T}$ is the area-averaged temperature for all measurement points (°C).

The heat removal efficiency (HRE) [16] reflects the energy utilization of a ventilation system, and indicates the temperature distribution uniformity and the performance in discharging contaminants. The calculation formula is:

$$\eta = \frac{T_e - T_s}{\overline{T_i} - T_s} \tag{10}$$

where T_e is the exhaust temperature (°C), T_s is the supply air temperature (°C), and $\overline{T_i}$ is the area-averaged temperature (°C).

The mean age of air [16] reflects the residence time of air in an airliner cabin and is calculated as follows:

$$\tau_i = \frac{\int_0^\infty c_i(t)dt}{c_i(0)} \tag{11}$$

where τ_i is the mean age of air (s), $c_i(t)$ is the SF_6 concentration at the measurement point (ppm), and $c_i(0)$ is the steady-state concentration at the beginning of the measurement (ppm).

2.4.2 Thermal comfort evaluation

Local thermal comfort in particular can reflect the influence of different parameters on passenger thermal comfort in airliner cabins [46]. Local thermal discomfort in airliner cabins is caused mainly by drafts and large vertical temperature differences between the head and ankles. These effects can be characterized by the draft rate (DR) and percentage dissatisfied (PD) [52].

The draft rate (DR) [53] can be calculated by formula (12):

$$DR = (34 - T_a) \cdot (u - 0.05)^{0.62} \cdot (0.37 \cdot u \cdot Tu + 3.14) \tag{12}$$

where T_a is the local air temperature (°C), u is the local mean air velocity (m/s), and Tu is the local turbulence intensity (%).

The percentage dissatisfied (PD), as a function of the vertical air temperature difference between the head and ankles, can be calculated by formula (13):

$$PD = \frac{100}{1 + exp(5.76 - 0.856 \cdot \triangle T_{a,v})} \tag{13}$$

where $\triangle T_{a,v}$ is the vertical air temperature difference between head and ankles (°C).

2.5 Health evaluation

In this study, the health evaluation was based on the COVID-19 infection risk. According to the Wells-Riley equation [54] and the particle concentration obtained from the experiments and simulations, the infection risk for passengers in airliner cabins can be estimated with the use of formula (14):

$$P = 1 - e^{(-C_i p t)} \tag{14}$$

where P is the infection risk for a passenger in an airliner cabin (-), C_i is the contaminant concentration (quantahour /m^3), p is the passenger's breathing flow rate (m^3/s), and t is the flight duration (s).

The quanta value [54] for COVID-19 can be estimated with the use of formula (15):

$$q = -\frac{Q ln(1 - P)}{I p t} \tag{15}$$

where q is the quanta value (/h), Q is the supply air volume (m^3/h), I is the number of index person (-).

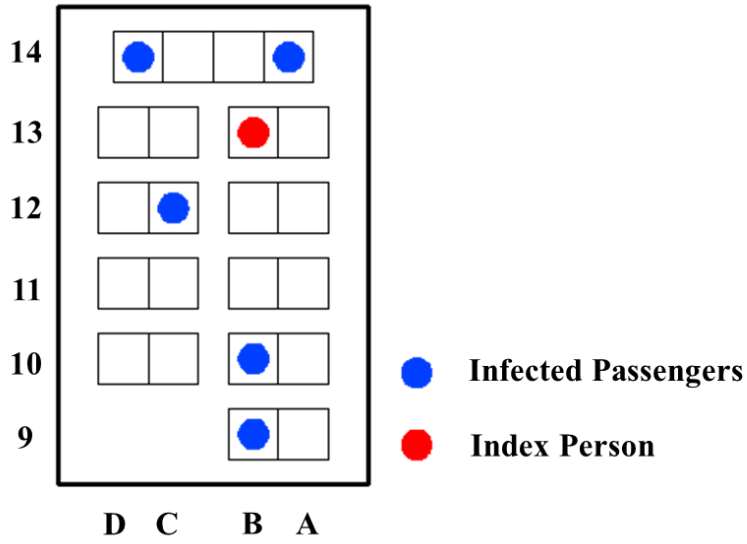

Figure 7 Schematic diagram of a section of a long-distance bus.

This study analyzed a case of COVID-19 transmission during a 2-hour bus ride [55] to determine the COVID-19 quanta value. Figure 7 is a schematic diagram of COVID-19 transmission inside the long-distance bus. The index person was located in seat 13B, the total number of infected passengers was 5, and the total infection risk was 5/22. The breathing flow rate for each passenger was set to 0.00053 m^3/s. The COVID-19 quanta value was inversely calculated as 29.8/h. A previous study showed that the COVID-19 quanta was between 14.0/h and 48.0/h [56]. This quanta value was applicable only for correcting the particle concentration in the measurement and may not represent the actual situation. In addition, we assumed that the duration of airliner flights was 3 hours (10800 s). In our simulation setup, the breathing area was a small box with a size of 20×20×20 cm^3 in front of the head of each dummy [57].

3. Results

3.1 Comfort evaluation

3.1.1 Airflow evaluation

Figure 8(a) and (b) display the VUI and TUI values, respectively, of the different air distribution systems. These values were calculated by the experiment results. The velocity and temperature were generally more uniform under the MV system than under DV. However, compared to cabin mockups in previous studies , the velocity and temperature uniformity of the DV system have been greatly improved [46].

Figure 8(c) shows the heat rejection efficiencies of the different air distribution systems. The HRE of direct ventilation systems was generally higher than that of mixed ventilation. However, compared with other cabin mockups in previous studies, the HRE of the MV system is greatly improved, possibly as a result of cabin mockups calibrating the air supply boundary which made the supply velocity uniform .

Figure 8(d) displays the mean age of air under the different air distribution systems. A previous study determined that the mean age of air in DV systems was significantly

lower than in MV systems [16]. However, in the present study the mean age of air under the MV system (with simultaneous supplies from the ceiling and sides of the cabin) did not differ greatly from that under the DV system.

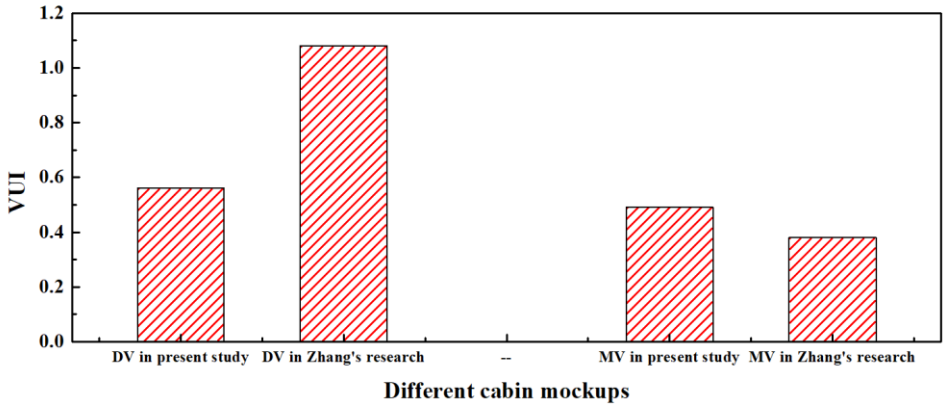

(a)

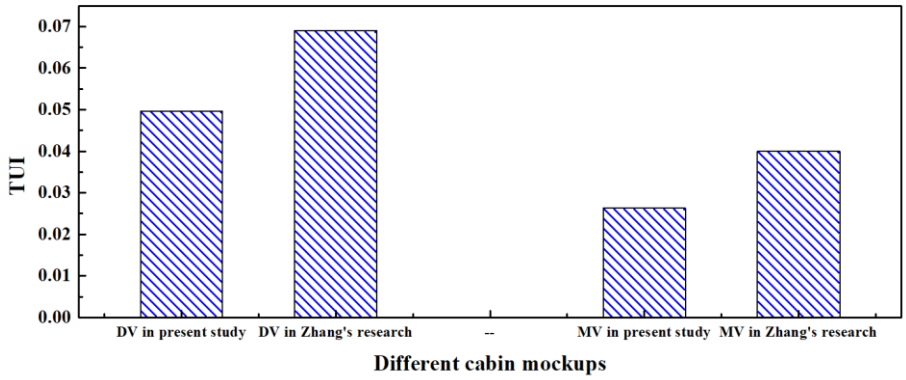

(b)

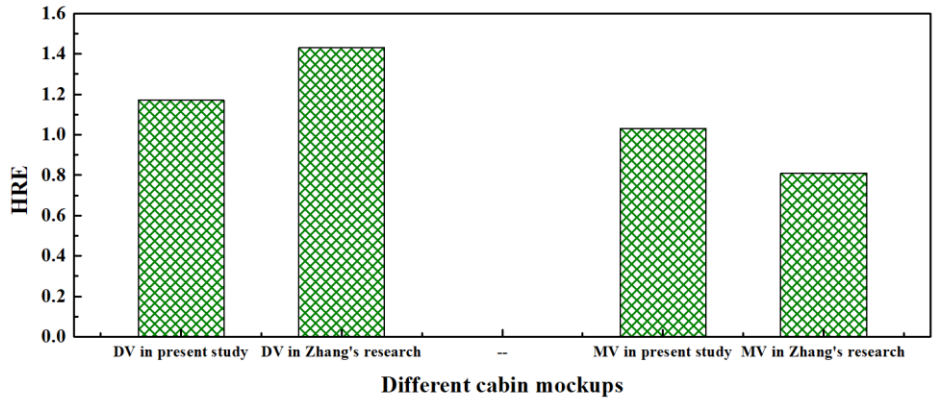

(c)

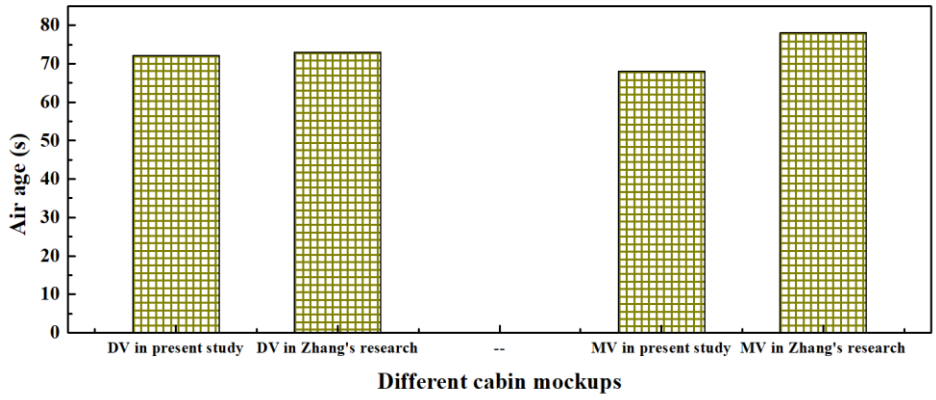

(d)

Figure 8 Comparisons of different air distribution systems in different cabin mockups. (a) VUIs, (b) TUIs, (c) HREs, and (d) mean age of air.

3.1.2 Thermal comfort evaluation

This study calculated the effects of drafts and vertical temperature differences on the thermal comfort of passengers under DV and MV systems and analyzed the DR and PD at 6 positions from A to F, as shown in Figure 9. The drafts that occurred with MV were strong. This was true especially for the seats near the aisle, where the draft rate reached 40%, possibly because the MV system in this study used supply air from the shoulder diffusers and ceiling diffusers simultaneously. The drafts that occurred with DV were basically small at each position, and the maximum draft rate (approximately 5%) was observed near the wall, possibly because this location was near the air supply diffusers. From the results of this study, we believe that the main reason for the discomfort of passengers under the MV system is drafts, whereas drafts have little effect on the thermal comfort of passengers under the DV system.

The two ventilation systems also produced significantly different temperature changes vertically from the head to the ankles. The reason for this result was the temperature stratification under the DV system and the relatively large temperature difference between head and ankles, whereas the temperature was more uniform under the MV system. From the results of this study, we believe that the main reason for the discomfort of passengers under the DV system is the excessive vertical temperature difference from the head to the ankles; in contrast, the vertical temperature difference had little effect on the thermal comfort of passengers under the MV system. If the head-ankle temperature difference can be kept sufficiently small, DV can maintain an acceptable thermal environment. This point of view is identical to that of Müller et al. [58].

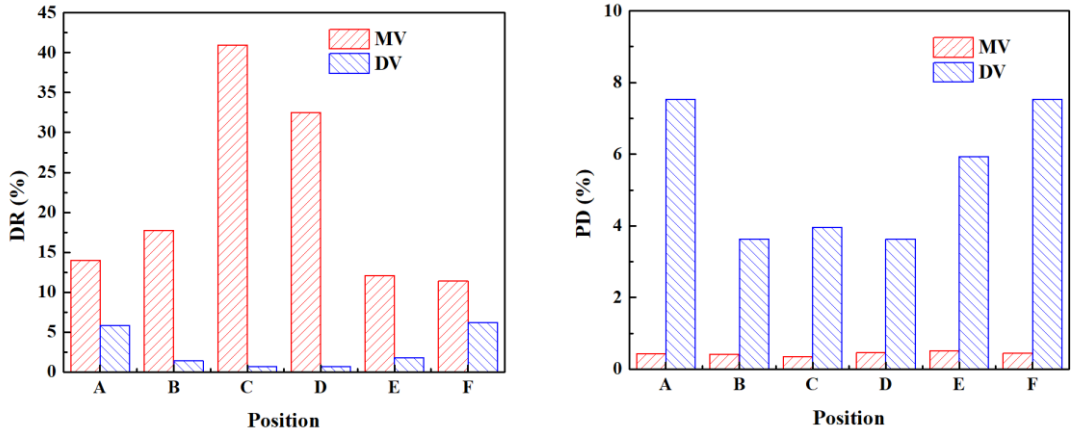

Figure 9 Local thermal discomfort under different air distribution systems: (a) draft risk and (b) percent dissatisfied.

3.2 Health evaluation

Figure 4 shows the air distributions in the cabin mockup with mixing and direct ventilation systems. In the MV system, the air jets from the shoulder diffusers were attached to the wall below the luggage racks before entering the main flow. The air distribution in the cross section was basically symmetrical, and two clockwise circulations formed on the left and right sides. These two circulations merged with the jets of the ceiling diffusers in the aisle, separated under the seats, and finally entered the air outlet along the floor. The presence of circulation will reduce the ventilation efficiency in the breathing region. In the center of the circulation area, low velocity was observed; this region was actually in a state of airflow stagnation. Compared to high-velocity areas, this area was obviously not conducive to the movement of air particles toward the exhaust outlet. In the DV system, most of the air flowed vertically upward from the floor of the aisle and directly exited through the ceiling diffuser.

The air distribution in an airliner cabin is related to the distribution of COVID-19 infection risk. The latter distribution was divided into three scenarios: no passengers wear masks, only the index passenger wears a mask, and all passengers wear masks.

3.2.1 No masks

Figure 10 shows the distribution of infection risks under the two ventilation systems when no passengers wear masks. Compared with other scenarios, under DV the highest average risk of infection for passengers appeared when the index person was located in seat C4. The average infection risk when the index person was located in seat B4 was slightly higher than that when the index person was in seat A4, and these two scenarios had significantly different distributions of the probability of infection risk for passengers. Under DV, in contrast, the influence of contaminants on passengers seated on the other side of the index person (Column D-E) was almost zero. The highest average risk of infection for passengers appeared when the index person was located in seat A4, and this

risk was significantly lower than the maximum risk of infection under MV. Since MV systems are widely used in airliners, it is not recommended that any passenger who may be an index person be seated in seats in Columns C or D, which are near the aisle, during the COVID-19 epidemic.

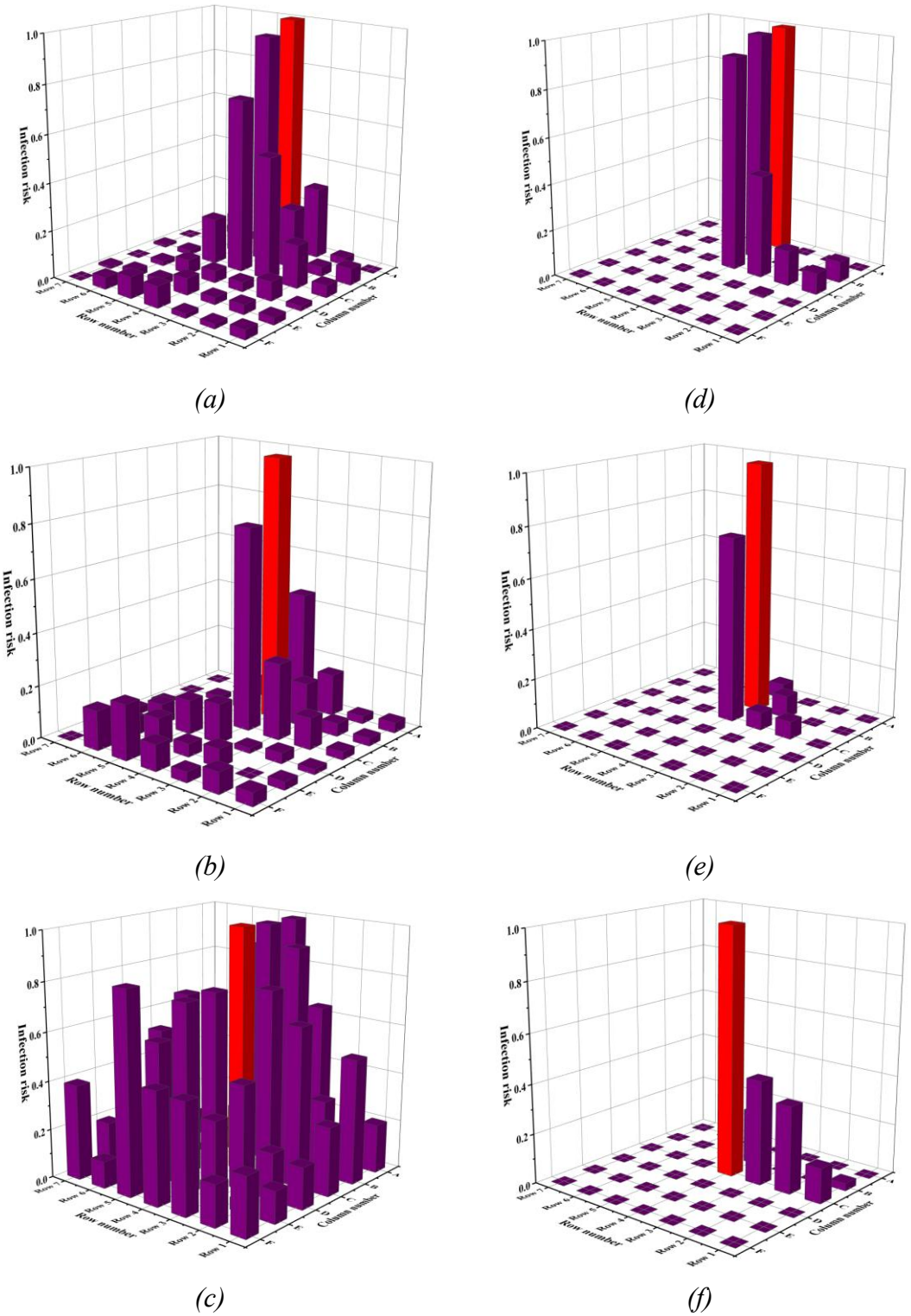

Figure 10 Infection risks when no passengers are wearing masks: (a) MV–A4, (b) MV–B4, (c) MV–C4, (d) DV–A4, (e) DV–B4 and (f) DV–C4.

3.2.2 Mask worn only by index person

Surgical-grade masks reduce the number of viruses in exhaled breath by 3.4 times [59]. Figure 11 displays the infection risks when the index person wears a mask. In this scenario, the risk of infection among adjacent passengers is significantly reduced, by up to 74%. Therefore, the wearing of a mask by the index person can effectively reduce the risk of infection for other passengers during the COVID-19 epidemic.

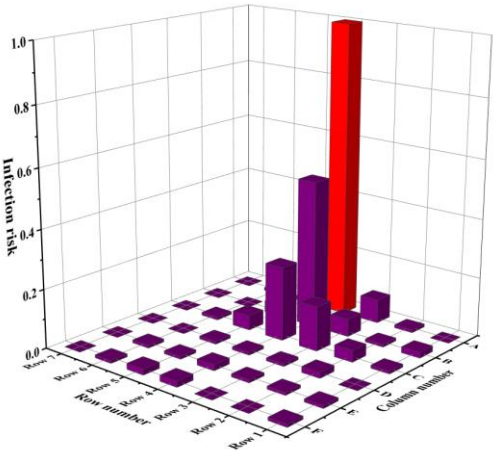

(a)

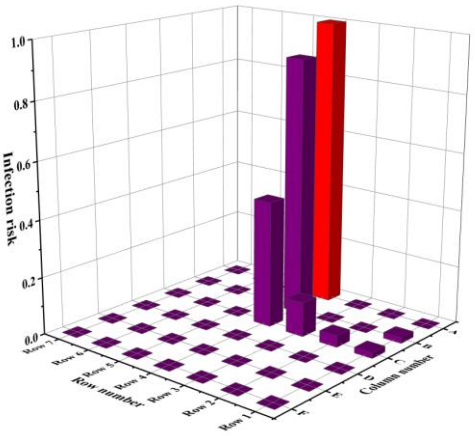

(d)

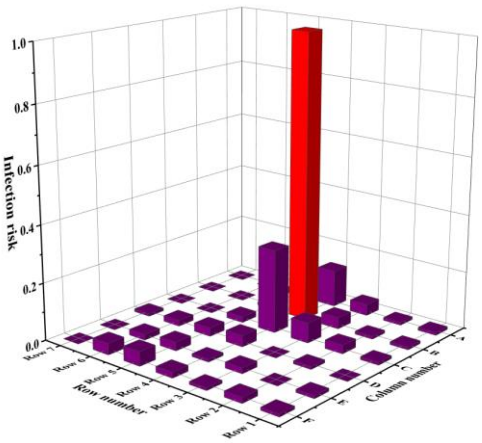

(b)

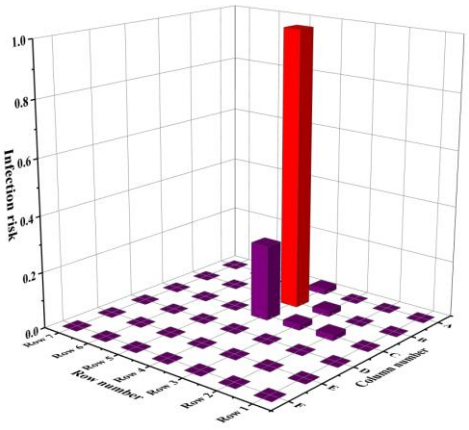

(e)

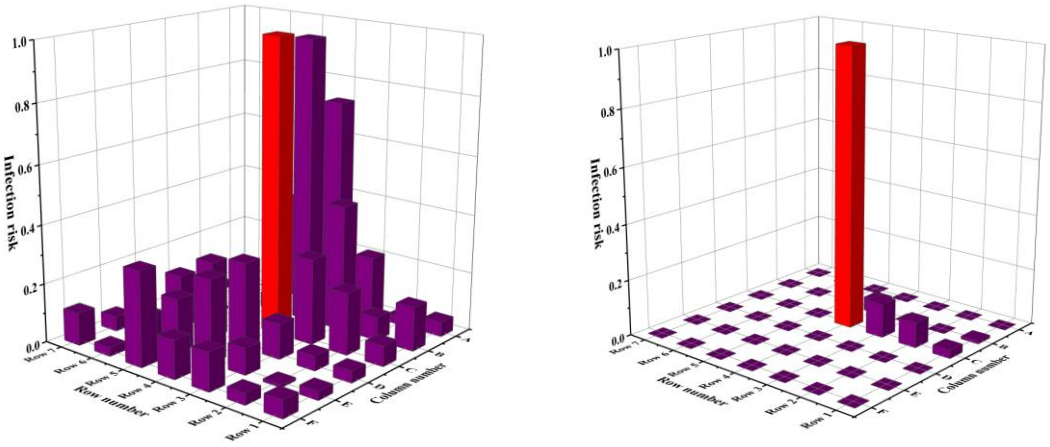

(c) *(f)*

Figure 11 Infection risks when only the index person wears a mask: (a) MV–A4, (b) MV–B4, (c) MV–C4, (d) DV–A4, (e) DV–B4 and (f) DV–C4.

3.2.3 Masks worn by all passengers

Figure 12 shows the infection risks under the two ventilation systems when all passengers wear masks. In this scenario, the risk of infection could decrease by up to 80%. Therefore, the wearing of masks can effectively reduce the probability of passenger infection during the COVID-19 epidemic.

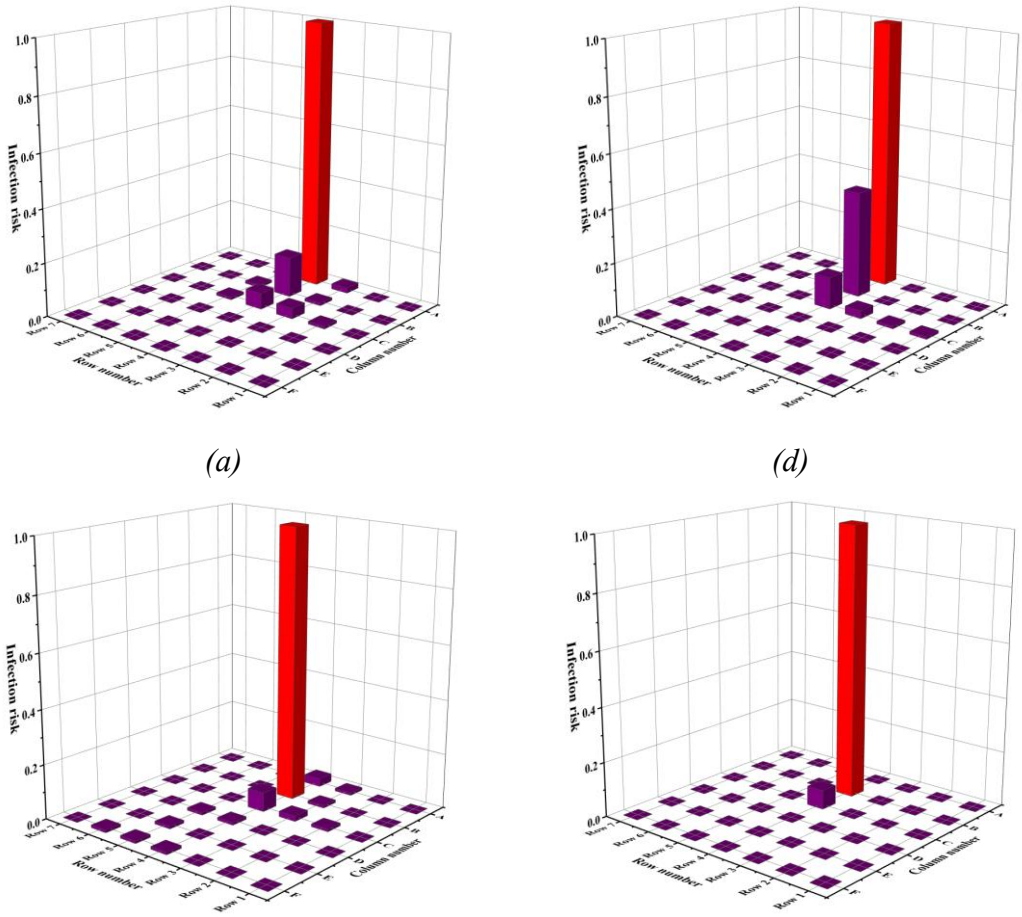

(a) *(d)*

(b) *(e)*

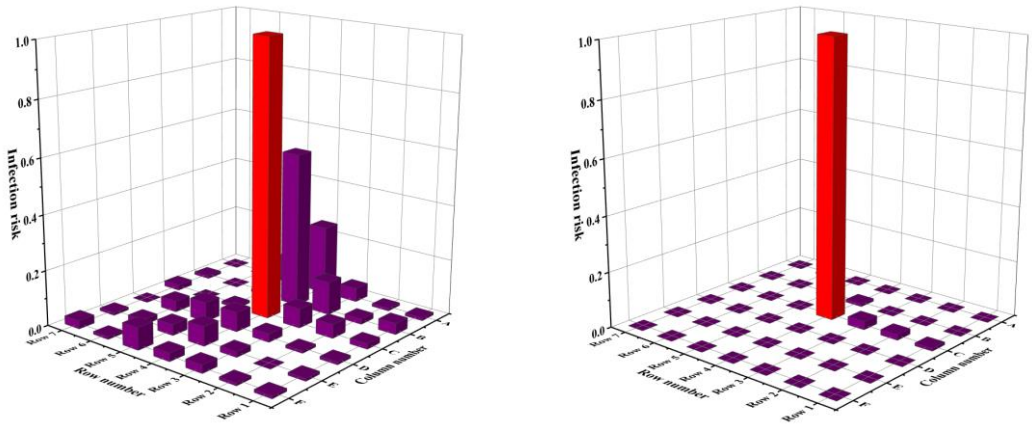

Figure 12 Infection risks when all passengers wear masks: (a) MV–A4, (b) MV–B4, (c) MV–C4, (d) DV–A4, (e) DV–B4, and (f) DV–C4.

The average infection risks for passengers in all scenarios are shown in Table 4. Under the MV system, the highest average risk of infection appeared when the index person was located in seat C4 near the aisle. In contrast, the highest average risk of infection under the DV system occurred when the index person was in seat A4 near the wall. When the index person wore a mask, the infection risk was reduced by an average of 65% under MV, and by an average of 60% under DV. When all passengers wore masks, the infection risk decreased further. Therefore, mask wearing is an effective method for preventing and controlling COVID-19 outbreaks. When all passengers wear masks, the infection risks under the DV and MV systems are similar, and mask wearing has a greater impact on infection risk with MV than with DV.

Table 4 *Infection risks under different air distribution systems*

Infection risk	MV			DV		
	No masks	Mask worn by index person only	Masks worn by all passengers	No masks	Mask worn by index person only	Masks worn by all passengers
A4	0.09	0.03	0.01	0.07	0.04	0.01
B4	0.11	0.03	0.01	0.04	0.01	0.00
C4	0.39	0.15	0.05	0.03	0.01	0.00
Average	0.20	0.07	0.02	0.05	0.02	0.00

4. Discussion

In a previous study, single-sized particles were used to calculate the infection risk in airliner cabins [26]. However, it has been shown that viruses are distributed differently on particles of different aerodynamic diameters. For example, another previous study found that 58% of influenza viruses were distributed on particles with an aerodynamic diameter ≥ 1 μm, and 42% on particles ≤ 1 μm [45]. Therefore, calculations with single-sized particles may be inaccurate.

In the present study, the calculations of infection risk with mixing ventilation were taken as an example. These calculations were divided into three operating scenarios: 1-μm particles, 5-μm particles, and mixed particles (1 μm, 5 μm). The results are displayed in Table 5, which was calculated by simulation results.

Table 5 *Average infection risk in the airliner cabin calculated for particles of different sizes under mixing ventilation*

	Monodisperse particles (1 μm)	Monodisperse particles (5 μm)	Polydisperse particles (1 μm and 5 μm)
A4	0.18	0.08	0.09
B4	0.14	0.09	0.11
C4	0.46	0.31	0.39

According to these results, the infection risk calculated for particles with an aerodynamic diameter of 1 μm is the highest, possibly because of the long diffusion range for the small-sized particles. The infection risk calculated for particles with an aerodynamic diameter of 5 μm was the lowest, and thus result may be related to the short diffusion range for the large-sized particles. The risk of infection calculated for polydisperse particles was between the risks for the other two scenarios. In fact, aerosols emitted by passengers cannot be monodisperse particles. Therefore, it is not accurate to calculate infection risk in airliner cabins using monodisperse particles; rather, polydisperse particles should be used.

To avoid an unfeasibly long experimental time, this study measured only a section of an airliner cabin with high infection risks and obtained the infection risk distributions for the entire section in order to verify the simulation model. In the future, the contaminant concentration distributions could be measured in different cross sections for verification of the COVID-19 infection risks obtained by these simulations in an airliner cabin. Furthermore, this paper focused only on the aerosol transmission of COVID-19. The virus can also be spread through droplets and skin contact, and pathogens deposited on surfaces may resuspend in the air and be inhaled by other passengers. These transmission channels in airliner cabins are worthy of further study. In addition, this paper mainly focused on the relative infection risks under the two ventilation systems. The operating scenario was one in which the passengers were sitting upright, and communication between passengers was not considered. The effects of activities (walking, talking etc.) among airline passengers on infection risk also merit further study.

5. Conclusions

Healthy and comfortable environments in the cabins of commercial airliners are essential for passengers and crew members. In this study, two air distribution systems (direct ventilation and mixing ventilation) were studied in a seven-row single-aisle airliner cabin mockup, and the risk of COVID-19 infection for passengers was evaluated with the use of the Wells-Riley equation. This investigation aimed to provide theoretical support for the choice of ventilation system in an airliner.

The main findings of the study are as follows.

1) There were advantages and disadvantages in terms of thermal comfort in both the DV and MV systems. Drafts affect the thermal comfort under MV, and an excessively high vertical temperature difference from head to ankles affects the thermal comfort under DV.
2) Although monodisperse particles were used in a previous study to calculate infection risk, polydisperse particles should be employed for more accurate calculation of the risk of infection in airliner cabins.
3) At the beginning of the epidemic, the infection risk under DV was lower than that under MV. However, in the middle and late stages of the epidemic, mask-wearing by passengers can greatly reduce the infection risk under MV, and it becomes approximately equal to the risk under DV.

Acknowledgements

This study was supported by the National Natural Science Foundation of China (NSFC) through grant No. 51978452 and No. 52108084. This study was partially supported by the China Postdoctoral Science Foundation through Grant No. 2020M680886.

References

[1] I. Baumann, M. Trimmel, Distribution of subjective assessments in a controlled aircraft environment, Aerospace Science & Technology 25(1) (2013) 93-101.
[2] Z. Zhang, X. Chen, S. Mazumdar, T. Zhang, Q. Chen, Experimental and numerical investigation of airflow and contaminant transport in an airliner cabin mockup, Building and Environment 44(1) (2009) 85-94.
[3] M. Liu, J. Liu, J. Ren, L. Liu, R. Chen, Y. Li, Bacterial community in commercial airliner cabins in China, International journal of environmental health research (2019) 1-12.
[4] M.R. Moser, T.R. Bender, H.S. Margolis, G.R. Noble, A.P. Kendal, D.G. Ritter, An outbreak of influenza aboard a commercial airliner, American Journal of Epidemiology (1) 1.
[5] T.A. Kenyon, S.E. Valway, W.W. Ihle, I.M. Onorato, K.G. Castro, Transmission of multidrug-resistant Mycobacterium tuberculosis during a long airplane flight, N Engl J Med 334(15) (1996) 933.
[6] S.J. Olsen, H.L. Chang, Y.Y. Cheung, F.Y. Tang, S.F. Dowell, Transmission of the Severe Acute Respiratory Syndrome on Aircraft, New England Journal of Medicine 349(25) (2004) 2416-2422.
[7] P. Christidis, A. Christodoulou, The predictive capacity of air travel patterns during the global spread of the COVID-19 pandemic: risk, uncertainty and randomness, International journal of environmental research and public health 17(10) (2020) 3356.
[8] L. Schibuola, C. Tambani, High energy efficiency ventilation to limit COVID-19

contagion in school environments, Energy and Buildings 240 (2021) 110882.
[9] P.S. Desai, N. Sawant, A. Keene, On COVID-19-safety ranking of seats in intercontinental commercial aircrafts: A preliminary multiphysics computational perspective, medRxiv (2020).
[10] D. Bhatia, A. De Santis, A preliminary numerical investigation of airborne droplet dispersion in aircraft cabins, Open Journal of Fluid Dynamics 10(3) (2020) 198-207.
[11] A.C. Davis, D.J. Menard, A.D. Clark, J.J. Cummins, N.A. Olson, Comparison of cough particle exposure for indoor commercial and aircraft cabin spaces, medRxiv (2021).
[12] K. Talaat, M. Abuhegazy, O.A. Mahfoze, O. Anderoglu, S.V. Poroseva, Simulation of aerosol transmission on a Boeing 737 airplane with intervention measures for COVID-19 mitigation, Physics of Fluids 33(3) (2021) 033312.
[13] R. You, Y. Zhang, X. Zhao, C.-H. Lin, D. Wei, J. Liu, Q. Chen, An innovative personalized displacement ventilation system for airliner cabins, Building and environment 137 (2018) 41-50.
[14] A.K. Melikov, Z.T. Ai, D.G. Markov, Intermittent occupancy combined with ventilation: An efficient strategy for the reduction of airborne transmission indoors, Science of The Total Environment 744 (2020) 140908.
[15] M.P. Wan, G.N. Sze To, C.Y.H. Chao, L. Fang, A. Melikov, Modeling the Fate of Expiratory Aerosols and the Associated Infection Risk in an Aircraft Cabin Environment, Aerosol Science & Technology 43(4) (2009) 322-343.
[16] Y. Zhang, J. Liu, J. Pei, J. Li, C. Wang, Performance evaluation of different air distribution systems in an aircraft cabin mockup, Aerospace Science and Technology 70 (2017) 359-366.
[17] Z. Tang, X. Cui, Y. Guo, N. Jiang, S. Dai, J. Liu, Near fields of gasper jet flows with wedged nozzle in aircraft cabin environment, Building and Environment 125(nov.) (2017) 99-110.
[18] J. Li, J. Liu, S. Dai, Y. Guo, N. Jiang, W. Yang, PIV experimental research on gasper jets interacting with the main ventilation in an aircraft cabin, Building and Environment 138 (2018) 149-159.
[19] S. Dai, H. Sun, W. Liu, Y. Guo, N. Jiang, J. Liu, Experimental study on characteristics of the jet flow from an aircraft gasper, Building and Environment 93 (2015) 278-284.
[20] B. Li, R. Duan, J. Li, Y. Huang, H. Yin, C.H. Lin, D. Wei, X. Shen, J. Liu, Q. Chen, Experimental studies of thermal environment and contaminant transport in a commercial aircraft cabin with gaspers on, Indoor air 26(5) (2016) 806-819.
[21] D. Al Assaad, C. Habchi, K. Ghali, N. Ghaddar, Simplified model for thermal comfort, IAQ and energy savings in rooms conditioned by displacement ventilation aided with transient personalized ventilation, Energy Conversion and Management 162(APR.) (2018) 203-217.
[22] J. Wang, G. Smedje, T. Nordquist, D. Norbaeck, Personal and demographic factors and change of subjective indoor air quality reported by school children in relation to exposure at Swedish schools: A 2-year longitudinal study, Science of the Total Environment 508(mar.1) (2015) 288-296.
[23] J.C.P.C. A, H.H.L.K. A, A.T.Y.L. B, J.C.K.T. C, A.K.H.L. B, Sensitivity analysis of

influence factors on multi-zone indoor airflow CFD simulation, Science of The Total Environment (2020).
[24] F. Berlanga, M.R. de Adana, I. Olmedo, J. Villafruela, J. San José, F. Castro, Experimental evaluation of thermal comfort, ventilation performance indices and exposure to airborne contaminant in an airborne infection isolation room equipped with a displacement air distribution system, Energy and Buildings 158 (2018) 209-221.
[25] D. Schmeling, J. Bosbach, Influence of shape and heat release of thermal passenger manikins on the performance of displacement ventilation in a train compartment, Indoor and Built Environment 29(6) (2020) 835-850.
[26] R. You, C.H. Lin, D. Wei, Q. Chen, Evaluating the commercial airliner cabin environment with different air distribution systems, Indoor air 29(5) (2019) 840-853.
[27] J. Maier, C. Marggraf-Micheel, T. Dehne, J. Bosbach, Thermal comfort of different displacement ventilation systems in an aircraft passenger cabin, Building & Environment 111(JAN.) (2017) 256-264.
[28] J. Maier, C. Marggraf-Micheel, F. Zinn, T. Dehne, J. Bosbach, Ceiling-based cabin displacement ventilation in an aircraft passenger cabin: Analysis of thermal comfort, Building and Environment 146(DEC.) (2018) 29-36.
[29] T. Zhang, Q. Chen, Novel air distribution systems for commercial aircraft cabins, Building & Environment 42(4) (2007) 1675-1684.
[30] Y. Yan, X. Li, Y. Shang, J. Tu, Evaluation of airborne disease infection risks in an airliner cabin using the Lagrangian-based Wells-Riley approach, Building and environment 121 (2017) 79-92.
[31] W. Liu, J. Wen, C.-H. Lin, J. Liu, Z. Long, Q. Chen, Evaluation of various categories of turbulence models for predicting air distribution in an airliner cabin, Building and Environment 65 (2013) 118-131.
[32] C. Wang, J. Liu, J. Li, F. Li, Chaotic behavior of human thermal plumes in an aircraft cabin mockup, International Journal of Heat and Mass Transfer 119 (2017).
[33] J. Bosbach, J. Pennecot, C. Wagner, M. Raffel, T. Lerche, S. Repp, Experimental and numerical simulations of turbulent ventilation in aircraft cabins, Energy 31(5) (2006) 694-705.
[34] M. Kühn, J. Bosbach, C. Wagner, Experimental parametric study of forced and mixed convection in a passenger aircraft cabin mock-up, Building and Environment 44(5) (2009) 961-970.
[35] C. Wang, J. Liu, J. Li, Y. Guo, N. Jiang, Turbulence characterization of instantaneous airflow in an aisle of an aircraft cabin mockup, Building & Environment 116 (2017) 207-217.
[36] F. Sanchez, S. Liscouet-Hanke, Thermal Risk Prediction Methodology for Conceptual Design of Aircraft Equipment Bays, Aerospace Science and Technology 104 (2020).
[37] G. Günther, J. Bosbach, J. Pennecot, C. Wagner, T. Lerche, I. Gores, Experimental and numerical simulations of idealized aircraft cabin flows, Aerospace Science and Technology 10(7) (2006) 563-573.
[38] Y. Liu, Q. Cao, W. Liu, C.-H. Lin, D. Wei, S. Baughcum, Z. Long, X. Shen, Q. Chen, Numerical modeling of particle deposition in the environmental control systems of

commercial airliners on ground, Building Simulation, Springer, 2017, pp. 265-275.
[39] B. Zhao, Y. Zhang, X. Li, X. Yang, D. Huang, Comparison of indoor aerosol particle concentration and deposition in different ventilated rooms by numerical method, Building & Environment 39(1) (2004) 1-8.
[40] M. Taheri, A. Zolfaghari, M. Afzalian, H. Hassanzadeh, The influence of air inlet angle in swirl diffusers of UFAD system on distribution and deposition of indoor particles, Building and Environment 191(107613) (2021) 1-13.
[41] J.K. Gupta, C.H. Lin, Q. Chen, Risk assessment of airborne infectious diseases in aircraft cabins, Indoor air 22(5) (2012) 388-395.
[42] W.L. Oberkampf, T.G. Trucano, Verification and validation in computational fluid dynamics, Progress in aerospace sciences 38(3) (2002) 209-272.
[43] W. Yan, Y. Zhang, Y. Sun, D. Li, Experimental and CFD study of unsteady airborne pollutant transport within an aircraft cabin mock-up, Building & Environment 44(1) (2009) 34-43.
[44] F. Li, J. Liu, J. Pei, C.H. Lin, Q. Chen, Experimental study of gaseous and particulate contaminants distribution in an aircraft cabin, Atmospheric Environment 85(MAR.) (2014) 223–233.
[45] J. Wei, Y. Li, Airborne spread of infectious agents in the indoor environment, American journal of infection control 44(9) (2016) S102-S108.
[46] M. Liu, D. Chang, J. Liu, S. Ji, C.-H. Lin, D. Wei, Z. Long, T. Zhang, X. Shen, Q. Cao, Experimental investigation of air distribution in an airliner cabin mockup with displacement ventilation, Building and Environment (2021) 107577.
[47] A.J. Mohr, Fate and transport of microorganisms in air, Manual of Environmental Microbiology, Third Edition, American Society of Microbiology2007, pp. 961-971.
[48] B. Ghosh, H. Lal, A. Srivastava, Review of bioaerosols in indoor environment with special reference to sampling, analysis and control mechanisms, Environment international 85 (2015) 254-272.
[49] Z.L. Qingyan Chen, Junjie Liu, Tengfei Zhang, Xiong Shen, Mingxin Liu, Qing Cao, Xingyang Li, Di Chang, Hanyu Li, Hongsheng Zhang, Xiaojing Zeng, Hao Zhang, High Quality Experimental Data of Particle Transport in Airliner Cabin, Tianjin University, 2020.
[50] Q. Cao, M. Liu, X. Li, C.-H. Lin, D. Wei, S. Ji, T. Zhang, Q. Chen, Influencing Factors in the Simulation of Airflow and Particle Transportation in Aircraft Cabins by CFD, Building and Environment (2021) 108413.
[51] T. Chen, S.-J. Cao, Numerical study on the integrated effects of supplied air velocity and exhaust velocity on particles removal for industrial buildings, Energy and Built Environment 2(4) (2021) 380-391.
[52] BSI, BS EN ISO 7730: 2005: Ergonomics of the Thermal Environment. Analytical Determination and Interpretation of Thermal Comfort Using Calculation of the PMV and PPD Indices and Local Thermal Comfort Criteria, International Standards Organization Geneva, 2005.
[53] X. Kong, C. Guo, Z. Lin, S. Duan, J. He, Y. Ren, J. Ren, Experimental study on the control effect of different ventilation systems on fine particles in a simulated hospital ward, Sustainable Cities and Society (2021) 103102.

[54] T. Lim, J. Cho, B.S. Kim, The predictions of infection risk of indoor airborne transmission of diseases in high-rise hospitals: Tracer gas simulation, Energy and Buildings 42(8) (2010) 1172-1181.
[55] Y.L. Jinming Shen, Is there a new transmission way of COVID-19?, 2020.
[56] H. Dai, B. Zhao, Association of the infection probability of COVID-19 with ventilation rates in confined spaces, Building Simulation, Springer, 2020, pp. 1321-1327.
[57] M. Ivanov, S. Mijorski, CFD modelling of flow interaction in the breathing zone of a virtual thermal manikin, Energy Procedia 112 (2017) 240-251.
[58] D. Müller, M. Schmidt, B. Müller, Application of a displacement ventilation system for air distribution in aircraft cabins, AST 2011 (2011).
[59] D.K. Milton, M.P. Fabian, B.J. Cowling, M.L. Grantham, J.J. McDevitt, Influenza virus aerosols in human exhaled breath: particle size, culturability, and effect of surgical masks, PLoS pathogens 9(3) (2013) e1003205.